



Showcasing research from Dr Enrico Iaccino and colleagues at the Department of Experimental and Clinical Medicine, University "Magna Graecia" of Catanzaro, Italy.

A novel phage display based platform for exosome diversity characterization

We applied the phage display approach to the E $\mu$ -Myc lymphoma preclinical model. After validating the phage binders' capability to target tumor mass and cells *in vivo* and *ex vivo*, we used phage binders to detect and trap the relative disease-derived exosomes from serum. Exosomes sorted by tumor-specific phage binders were analyzed for their miRNA content compared to exosomes isolated with conventional reagents. As a result, phage-positive exosomes revealed an independent mirnomic signature with respect to the conventional isolated exosomes. The cover image has been realized by Ella Maru Studio (<https://scientific-illustrations.com/>).

As featured in:



See Sebastiano Andò, Enrico Iaccino *et al.*, *Nanoscale*, 2022, 14, 2998.



Cite this: *Nanoscale*, 2022, **14**, 2998

Received 14th October 2021,

Accepted 4th January 2022

DOI: 10.1039/d1nr06804k

rs.c.li/nanoscale

## A novel phage display based platform for exosome diversity characterization†

Domenico Maisano,<sup>†</sup> Selena Mimmi,<sup>‡</sup> Vincenzo Dattilo,<sup>b</sup> Fabiola Marino,<sup>a</sup> Massimo Gentile,<sup>c</sup> Eleonora Vecchio,<sup>a</sup> Giuseppe Fiume,<sup>a</sup> Nancy Nisticò,<sup>a</sup> Annamaria Aloisio,<sup>a</sup> Maria Penelope de Santo,<sup>d</sup> Giovanni Desiderio,<sup>d</sup> Vincenzo Musolino,<sup>e</sup> Saverio Nucera,<sup>e</sup> Francesca Sbrana,<sup>f</sup> Sebastiano Andò,<sup>\*g</sup> Simone Ferrero,<sup>h</sup> Andrea Morandi,<sup>i</sup> Francesco Bertoni,<sup>j</sup> Ileana Quinto<sup>§a</sup> and Enrico Iaccino<sup>\*§a</sup>

**We present an innovative approach allowing the identification, isolation, and molecular characterization of disease-related exosomes based on their different antigenic reactivities. The designed strategy could be immediately translated into any disease in which exosomes are involved. The identification of specific markers and their subsequent association with exosome subtypes, together with the possibility to engineer target-guided exosome-like particles, could represent the key for the effective adoption of exosomes in clinical practice.**

The common approach in oncology diagnosis is currently represented by tissue biopsy, which over time has managed to earn the title of “gold standard” for microscopic and macroscopic examination of tumor tissues together with radio imaging-based investigations.<sup>1</sup> Even though tissue biopsies represent a truthful tool in cancer detection and, despite the successes that this technique has accumulated over the years it remains very invasive and risky for the patient.<sup>2</sup> In addition to invasiveness, which in some cases can cause negative impli-

cations from a clinical point of view,<sup>3,4</sup> one of the major problems, and above all relating to small tumor masses, lies precisely in the impossibility, for tissue biopsy, to provide a wide assessment of tumor heterogeneity.<sup>5</sup>

A large contribution in the analysis of tumor heterogeneity, mostly considering the neoplasm in its continuous molecular evolution, is currently provided by the liquid biopsy.<sup>6</sup> In fact, taking into consideration the circulating tumor components in blood vessels and body fluids – known as the tumor circulome<sup>7</sup> – liquid biopsy aims to provide significant information about tumor dynamism, managing in many cases to anticipate the still-in-use prognostic and diagnostic approaches,<sup>8</sup> always in association with the common investigation techniques in oncology.

Exosomes are a subtype of extracellular vesicles (EV), 30–150 nm in diameter, with an essential role as mediators of both physiological and pathological processes, including cancer,<sup>9</sup> neurodegenerative diseases,<sup>10</sup> and cardiovascular disease.<sup>11</sup> Together with their cargo of proteins, nucleic acids, and lipids, exosomes are secreted through endosome-mediated exocytosis by all cells and widely released in the blood, urine, cerebrospinal fluid, and other body fluids.<sup>9,12,13</sup> Due to these features, exosomes are potentially capable of capturing the different biological properties associated with pathological alterations and could be used to design innovative biomarkers for longitudinal measures during disease progression, particularly relevant for those diseases in which early detection could significantly impact disease prognosis. Indeed, representing a molecular footprint of the cell of origin, exosomes are considered a promising tool to design reliable liquid biopsy options for non-invasive monitoring of disease evolution, recurrence, and response to therapy.<sup>14,15</sup>

In the last decade, a wide array of efficient protocols for exosome purification have been published but none of them allows the association of a specific marker with an exosome subtype and the exosome subtype with a particular function and/or group of functions.<sup>16–18</sup> Indeed, the current standards

<sup>a</sup>Department of Experimental and Clinical Medicine, University “Magna Graecia of Catanzaro”, Catanzaro, Italy. E-mail: iaccino@unicz.it

<sup>b</sup>Genetics Units, IRCCS Centro San Giovanni di Dio Fatebenefratelli, Brescia, Italy

<sup>c</sup>Hematology Unit, Annunziata Hospital, Cosenza, Italy

<sup>d</sup>CNR/Nanotec, Physics Department, University of Calabria, Rende, CS, Italy

<sup>e</sup>IRC-FSH Department of Health Sciences, University “Magna Graecia” of Catanzaro, Catanzaro, Italy

<sup>f</sup>Schaefer SEE srl, Via Luigi Einaudi 23, Rovigo, RO, Italy

<sup>g</sup>Health Center, University of Calabria, Rende, CS, Italy.

E-mail: sebastiano.ando@unical.it

<sup>h</sup>Division of Hematology, Department of Molecular Biotechnologies and Health Sciences, University of Torino, Turin, Italy

<sup>i</sup>Department of Experimental and Clinical Biomedical Sciences, University of Florence, Florence, Italy

<sup>j</sup>IOR, Institute of Oncology Research, Faculty of Biomedical Sciences, USI, Bellinzona, Switzerland

†Electronic supplementary information (ESI) available. See DOI: 10.1039/d1nr06804k

‡These authors shared first authorship.

§These authors shared senior authorship.

for exosome characterization are largely based on the adoption of a set of markers that, similarly to those used in the identification of stem cells, can heavily differ among different tumor types and genetic backgrounds.<sup>19</sup>

Here, we describe an innovative method that is not based on *a priori* definition of exosome-associated markers by applying a phage display approach to a preclinical model of hematological malignancy, used as a proof of principle. Phage display

is a powerful tool that allows the identification and the isolation of peptides with high affinity and specificity by a target-guided selective pressure.<sup>20</sup> During the last few years, we successfully validated the screening of random peptide libraries (RPLs) as a method to identify phage-derived peptide binders for the idiotypic determinants of the immunoglobulin B cell receptors (IgBCRs).<sup>21–23</sup> Using a multiple myeloma preclinical model, we demonstrated that tumor B cell-derived exosomes

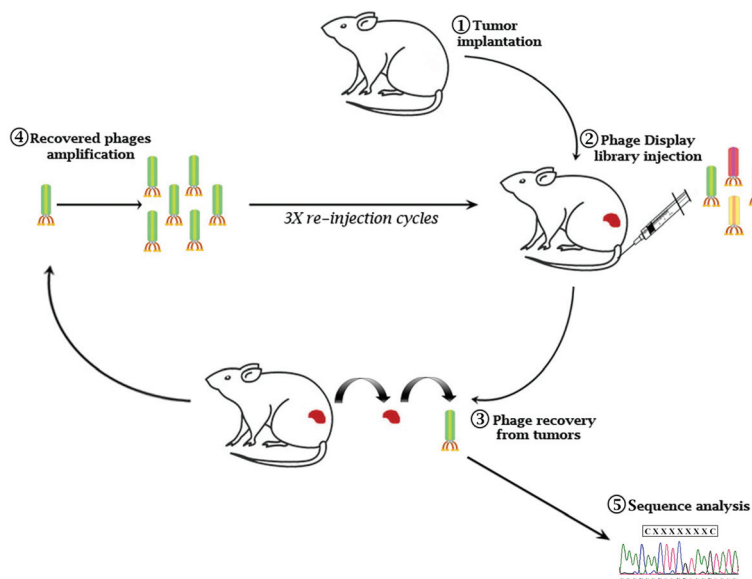


**Fig. 1** Workflow of the *in vivo* phage display screening. (1) E $\mu$ -myc-derived cells ( $1 \times 10^6$  cells) were subcutaneously (s.v.) injected in the mice. (2) 10  $\mu$ l of Ph.D.-C7C phage display peptide library was directly injected into the tail vein of mice bearing a palpable E $\mu$ -myc-derived tumor mass on the flank (5–6 mm in maximal diameter). (3) Tumor masses were collected, and phages were recovered through acidic elution. (4) The eluted phages were amplified by infecting *Escherichia coli* and used for the following cycle of selection. (5) Ultimately, the DNA of the isolated phage clones was sequenced to determine the amino acid sequence of the insert.

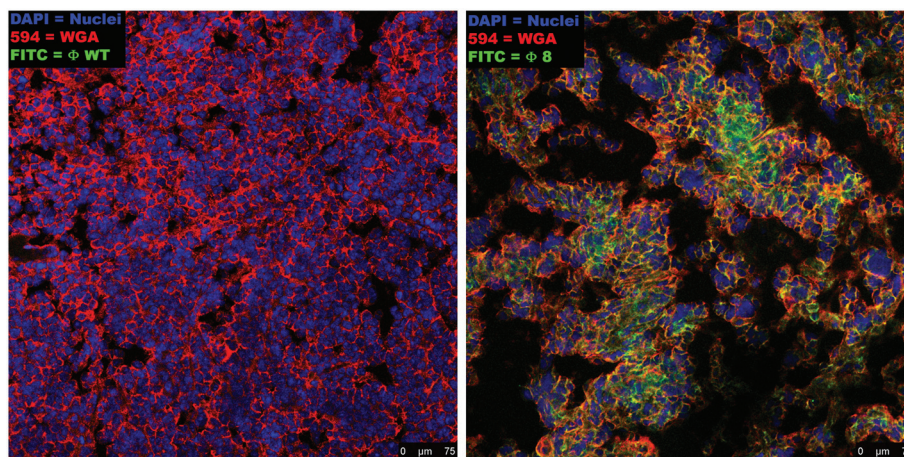


**Fig. 2** *Ex vivo* tumor-specific targeting of selected phage ligands. The representative confocal images were derived from the OCT-embedded tissue samples from the tumor-harboring mice cut in 8–10  $\mu$ m sections. Therefore, areas not perfectly under focus are correlated with the section thickness. Moreover, from each sample, we selected the more representative images of multiple serial cross-sections. Non-specific binding can be excluded given the absence of the FITC signal in the sections incubated with the wild-type phage (on the left) with respect to the ones incubated with the tumor-specific  $\Phi$ 8 (right panel). Confocal images were acquired at the same magnification as shown in the figure (scale bar = 75  $\mu$ m).

express the IgBCR of their parental malignant B-cells, thus constituting a personal “barcode” of tumor clones, which can be subsequently targeted by the idiotypic specific binders.<sup>8</sup>

Unlike our previous works in which we used the IgBCRs as bait for the screening, to verify the suitability of this techno-

logy even in the absence of an unequivocal exosome marker, in this work we adopted E $\mu$ -myc transgenic mice lacking immunoglobulin expression.<sup>24</sup>

E $\mu$ -myc B-lymphoma cells were isolated from the tumor mass of E $\mu$ -myc tumor-bearing mice and subcutaneously re-inoculated into wild-type syngeneic mice (ESI Fig. 1A†). After 4 cycles of reinoculation, we established an E $\mu$ -myc B-lymphoma xenograft model with homogeneous phenotypic characteristics in terms of the survival rate and time of tumor onset (ESI Fig. 1B and C†). A constrained random phage display library (CX7C) was intravenously injected into E $\mu$ -myc tumor-bearing mice. After 1 hour of circulation, the mice were perfused to remove nonspecific binders. Tumor tissues were collected, phages from the tumor mass were amplified and used for the following cycles of selection (Fig. 1). After three biopanning cycles, 20 independent phages were randomly chosen to retrieve the selected epitopes' amino acid sequence (ESI Table 1†). To verify the tumor specificity of the clones, phages were conjugated with fluorescein isothiocyanate (FITC) as a fluorophore and used in the cytofluorimetric analysis (ESI Fig. 2†). Based on the percentage of clonal identity and the high-affinity binding to target tumor cells, phage clone 8 (CNAGHLSQC) was chosen for further characterization studies.

The binding of the selected phage ( $\Phi$ 8) to the target tumor cells was identified by confocal analysis of the sections of fresh tumor tissues stained with  $\Phi$ 8-FITC conjugated, demonstrating a clear overlap of the signal derived from  $\Phi$ 8-FITC (green) and that of wheat germ agglutinin staining (red) directed against glycoproteins of the cancer cells within the tumor mass (Fig. 2). Wild-type (WT) phage was used as a control and no fluorescence signal was recorded.



**Fig. 3** *In vivo* targeting and biodistribution of FITC-conjugated phage clones. FITC-conjugated phage particles were intravenously administered in tumor-harboring mice and healthy control. After 2 hours of circulation, animals were anesthetized and fluorescence was measured using a Bruker *In vivo* Xtreme X-ray/optical imaging system. Images were acquired demonstrating a clear fluorescence accumulation into the tumor mass of FITC-conjugated  $\Phi$ 8 recipients with respect to the wild-type recipients and to the tumor-free control.



**Fig. 4** *In vitro* validation and characterization of exosome preparations. (A) Size distribution and the concentration of EV particles were determined by the tunable resistive pulse sensing (TRPS) method (qNano, Izon Science Ltd). The size distribution has a mean value of 125 nm (St. dev 32.2 nm), and the solution has a concentration of  $3 \times 10^{10}$  particles per ml. (B) Flow cytometric analysis of exosomes derived from the serum of representative E $\mu$ -myc mice incubated with the FITC-conjugated bacteriophage  $\Phi$ 8. First, total exosomes were purified by the standard purification protocol based on size exclusion chromatography. Then, the exosomes derived from the different preparations (control and E $\mu$ -myc-derived exosomes) were stained with  $\Phi$ 8 (green) and analyzed using a BD FACSCanto II flow cytometer. Exosomes were gated in FSC-A vs. SSC-A. Stringent gating strategies to exclude debris that exhibit autofluorescence were applied. The mean fluorescence intensity (MFI) was evaluated using FlowJo software and represented as a histogram including ten independent replicates.



**Fig. 5** Microscopy analysis of bacteriophage-mediated exosome trapping. Topographic images of the bacteriophage coated samples (left), the phage incubated with control exosomes (center) and the phage incubated with Em-myc exosomes (right). Images were acquired by atomic force microscopy in tapping mode in air (top panels) and environmental scanning electron microscopy in low vacuum (bottom panels). Both techniques show an enrichment of E $\mu$ -myc derived exosomes with respect to those incubated with tumor-free derived exosomes.

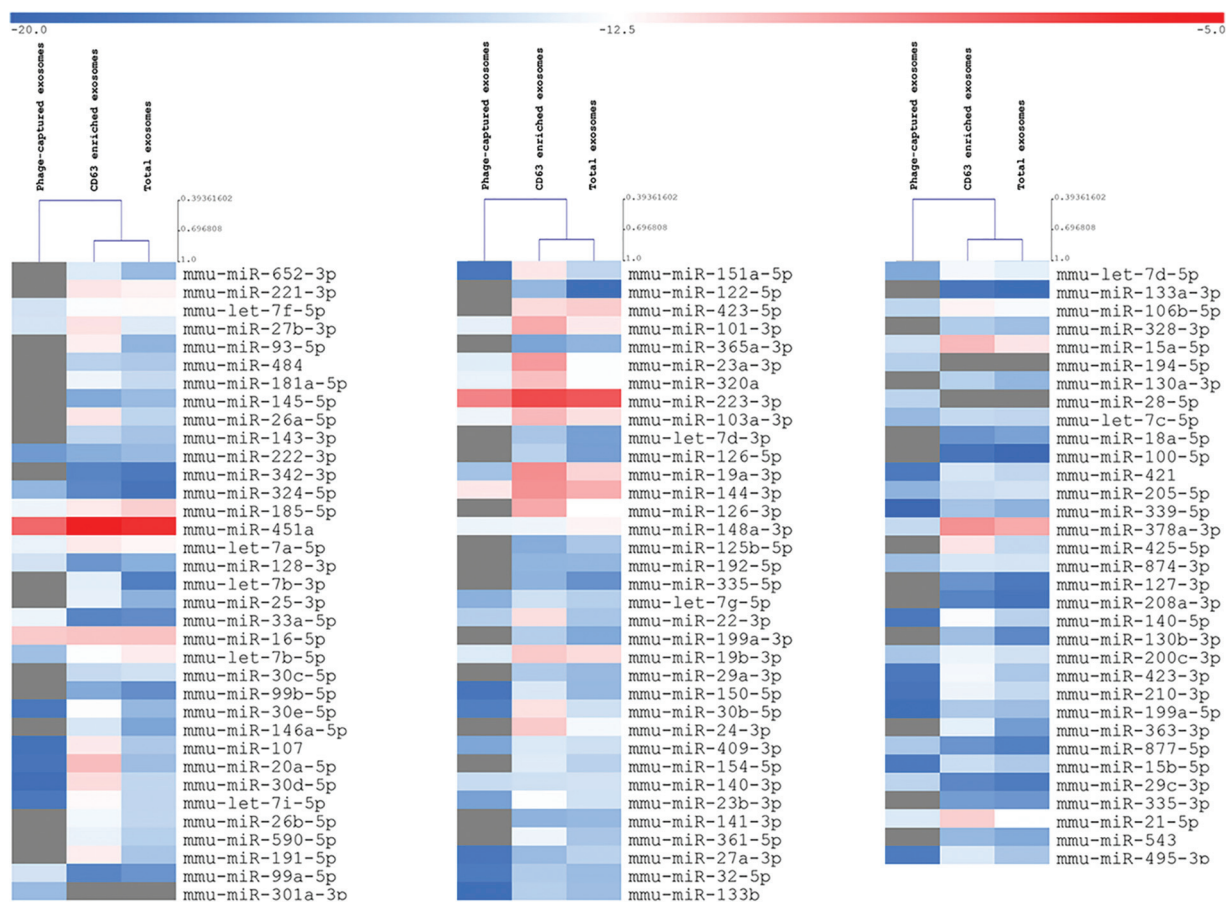


**Fig. 6** Heat map of differentially expressed miRNAs in exosome subpopulations. The biotin-conjugated  $\Phi 8$  bacteriophage was used to trap and molecularly characterize an E $\mu$ -myc-derived exosome subpopulation and analyzed in comparison with both CD63-sorted and total exosome counterparts. Data are represented as normalized values ( $\Delta C_t = \text{cel-miR-39-3p}, C_t - \text{target miRNA } C_t$ ) and the intensity plot (top bar) shows the relative up-regulation (red) and down-regulation (blue).

The  $\Phi 8$ -mediated tumor-specific targeting was also *in vivo* validated, phages were again used in combination with FITC for conjugating to primary amines on the phage proteins and used as a probe. Phage particles were intravenously administered, and after 2 hours of circulation, conversely to the controls, an evident accumulation of fluorescence in  $E\mu$ -myc subcutaneously tumor-bearing mice was seen in  $\Phi 8$  FITC-conjugated recipients (Fig. 3).

Based on these positive results, we aim to validate this approach for the identification and selection of cancer-released exosomes. After a preliminary exosome purification protocol based on size exclusion chromatography (Fig. 4A), we tested the ability of phage 8 in exosomes detection. In contrast to the exosomes purified from control mice, FACS analysis identified a distinct  $\Phi 8$  FITC-conjugated positive exosome subpopulation in the exosome preparations derived from the  $E\mu$ -myc-derived exosomes (Fig. 4B).

Encouraged by these pieces of evidence, and to validate the potential phage-mediated exosome trapping ability, we performed a preliminary bacteriophage coating of atomically flat substrates followed by a short incubation with the target exosomes. Both atomic force microscopy (AFM) and environmental scanning electron microscopy (ESEM) showed an appreciable enrichment of  $E\mu$ -myc derived exosomes with respect to those incubated with tumor-free derived exosomes and to the substrates coated with the WT phage (Fig. 5).

To verify whether the described approach could satisfy the need for reliable technologies for the molecular characterization of disease-related exosome subcategories, we lastly analyzed three differently sorted exosome subpopulations (total, CD63,  $\Phi 8$ ) by qRT-PCR analysis of a predefined set of miRNAs that were reported to be associated with exosomes.

Even if not directly addressed to identify the expression levels of miRNAs, the analysis results highlighted the deregulation of crucial tumor progression, invasion, and proliferation players such as miR-15a,<sup>25</sup> miR33a-5p,<sup>26</sup> and miR-151a-5p.<sup>27</sup> The unsupervised hierarchical clustering showed that the total and CD63 positive exosomes demonstrated substantial uniform expression levels of miRNAs, whereas exosomes sorted for their affinity to  $\Phi 8$  showed an independent exosome-derived miRNA profile (Fig. 6).

## Conclusions

We described a proof-of-principle approach of phage display technology as a tool for the identification and isolation of disease-related exosomes. In this regard, phage-based technology could be crucial in the era of personalized therapy. Indeed, the majority of neoantigens should arise from random, spontaneous mutations with little overlap between individual patients. Such a “private” antigen expression indicates the need for a personal biopanning procedure making the proposed model a potentially revolutionary approach. Adapting our validated approach to the enormous possibilities given by the use of patient-derived xenograft (PDX), the

reported *in vivo* phage-display-based platform could represent the cornerstone for a comprehensive molecular characterization of disease-related exosomes. Capturing the biological implications of exosome production and release in different pathological contexts could be useful for further describing innovative biomarker nanotechnological platforms to be applied to diseases in which exosomes play a role, such as cancer and neurodegenerative disorders, and greatly impacting the new era of liquid biopsy.

## Author contributions

Conceptualization: EI, SM, DM, and IQ; methodology: DM, SM, FB, EV, GF, NN, AA, MPDS, GD, VM, MG, SN, and FS; investigation: DM, SM, VD, FB, EV, GF, NN, AA, MPDS, GD, VM, MG, SN, and FS; funding acquisition: EI, SM, DM, and IQ; supervision: EI, SM, and IQ; writing – the original draft: EI; and writing – review and editing: AM, SF, SA, FB, IQ, and VM.

## Conflicts of interest

There are no conflicts to declare.

## Acknowledgements

This work was supported by the following grants: MIUR-PRIN 2017MHJJ55\_002 to IQ; GILEAD Fellowship 2018 to EI; EU PON Salute ARS01\_00568 to S.A; POR FES/FESR 2014-20-ATS ALCMEONE cup J18C17000610006 to IQ.

## Notes and references

- 1 H. Liu, M. Ruan, H. Wang, H. Wang, X. Li and G. Song, Can fewer transperineal systematic biopsy cores have the same prostate cancer detection rate as of magnetic resonance imaging/ultrasound fusion biopsy?, *Prostate Cancer Prostatic Dis.*, 2020, **23**, 589–595.
- 2 J. Marrugo-Ramírez, M. Mir and J. Samitier, Blood-based cancer biomarkers in liquid biopsy: A promising non-invasive alternative to tissue biopsy, *Int. J. Mol. Sci.*, 2018, **19**, 2877.
- 3 M. J. Resnick, D. J. Lee, L. Magerfleisch, K. N. Vanarsdalen, J. E. Tomaszewski, A. J. Wein, S. B. Malkowicz and T. J. Guzzo, Repeat prostate biopsy and the incremental risk of clinically insignificant prostate cancer, *Urology*, 2011, **77**, 548–552.
- 4 K. Shyamala, H. C. Girish and S. Murgod, Risk of tumor cell seeding through biopsy and aspiration cytology, *J. Int. Soc. Prev. Community Dent.*, 2014, **4**, 5–11.
- 5 H. M. Huang and H. X. Li, Tumor heterogeneity and the potential role of liquid biopsy in bladder cancer, *Cancer Commun.*, 2021, **41**, 91–108.

- 6 M. Russano, A. Napolitano, G. Ribelli, M. Iuliani, S. Simonetti, F. Citarella, F. Pantano, E. Dell'Aquila, C. Anesi, N. Silvestris, A. Argentiero, A. G. Solimando, B. Vincenzi, G. Tonini and D. Santini, Liquid biopsy and tumor heterogeneity in metastatic solid tumors: the potentiality of blood samples, *J. Exp. Clin. Cancer Res.*, 2020, **39**, 95.
- 7 J. Wu, S. Hu, L. Zhang, L. Xin, C. Sun, L. Wang, K. Ding and B. Wang, Tumor circulome in the liquid biopsies for cancer diagnosis and prognosis, *Theranostics*, 2020, **10**, 4544–4556.
- 8 E. Iaccino, S. Mimmi, V. Dattilo, F. Marino, P. Candeloro, A. Di Loria, D. Marimpietri, A. Pisano, F. Albano, E. Vecchio, S. Ceglia, G. Golino, A. Lupia, G. Fiume, I. Quinto and G. Scala, Monitoring multiple myeloma by idiotypic specific peptide binders of tumor-derived exosomes, *Mol. Cancer*, 2000, **16**, 159.
- 9 R. Kalluri, The biology and function of exosomes in cancer, *J. Clin. Invest.*, 2016, **26**, 1208–1215.
- 10 Y. Men, J. Yelick, S. Jin, Y. Tian, M. S. R. Chiang, H. Higashimori, E. Brown, R. Jarvis and Y. Yang, Exosome reporter mice reveal the involvement of exosomes in mediating neuron to astroglia communication in the CNS, *Nat. Commun.*, 2019, **10**, 4136.
- 11 A. Ibrahim and E. Marbán, Exosomes: Fundamental Biology and Roles in Cardiovascular Physiology, *Annu. Rev. Physiol.*, 2016, **78**, 67–83.
- 12 R. Kalluri and V. S. LeBleu, The biology, function, and biomedical applications of exosomes, *Science*, 2020, **367**, eaau6977.
- 13 M. Mathieu, L. Martin-Jaular, G. Lavieu and C. Théry, Specificities of secretion and uptake of exosomes and other extracellular vesicles for cell-to-cell communication, *Nat. Cell Biol.*, 2019, **21**, 9–17.
- 14 T. B. Steinbichler, J. Dudás, H. Riechelmann and I. I. Skvortsova, The role of exosomes in cancer metastasis, *Semin. Cancer Biol.*, 2017, **44**, 170–181.
- 15 G. De Rubis, S. Rajeev Krishnan and M. Bebawy, Liquid Biopsies in Cancer Diagnosis, Monitoring, and Prognosis, *Trends Pharmacol. Sci.*, 2019, **40**, 172–186.
- 16 M. Tkach, J. Kowal and C. Théry, Why the need and how to approach the functional diversity of extracellular vesicles, *Philos. Trans. R. Soc. London, Ser. B*, 2018, **373**, 20160479.
- 17 R. Crescitelli, C. Lässer and J. Lötvall, Isolation and characterization of extracellular vesicle subpopulations from tissues, *Nat. Protoc.*, 2021, **16**(3), 1548–1580.
- 18 Y. Chen, Q. Zhu, L. Cheng, Y. Wang, M. Li, Q. Yang, L. Hu, D. Lou, J. Li, X. Dong, L. P. Lee and F. Liu, Exosome detection via the ultrafast isolation system: EXODUS, *Nat. Methods*, 2021, **18**, 212–218.
- 19 I. Manna, E. Iaccino, V. Dattilo, S. Barone, E. Vecchio, S. Mimmi, E. Filippelli, G. Demonte, S. Polidoro, A. Granata, S. Scannapieco, I. Quinto, P. Valentino and A. Quattrone, Exosome-associated miRNA profile as a prognostic tool for therapy response monitoring in multiple sclerosis patients, *FASEB J.*, 2018, **32**, 4241–4246.
- 20 S. Mimmi, D. Maisano, I. Quinto and E. Iaccino, Phage Display: An Overview in Context to Drug Discovery, *Trends Pharmacol. Sci.*, 2019, **40**, 87–91.
- 21 C. Palmieri, C. Falcone, E. Iaccino, F. M. Tuccillo, M. Gaspari, F. Trimboli, A. De Laurentiis, L. Luberto, M. Pontoriero, A. Pisano, E. Vecchio, O. Fierro, M. R. Panico, M. Larobina, S. Gargiulo, N. Costa, F. Dal Piaz, M. Schiavone, C. Arra, A. Giudice, G. Palma, A. Barbieri, I. Quinto and G. Scala, In vivo targeting and growth inhibition of the A20 murine B-cell lymphoma by an idiotypic-specific peptide binder, *Blood*, 2010, **116**, 226–238.
- 22 S. Mimmi, E. Vecchio, E. Iaccino, M. Rossi, A. Lupia, F. Albano, F. Chiurazzi, G. Fiume, A. Pisano, S. Ceglia, M. Pontoriero, G. Golino, P. Tassone, I. Quinto, G. Scala and C. Palmieri, Evidence of shared epitopic reactivity among independent B-cell clones in chronic lymphocytic leukemia patients, *Leukemia*, 2016, **30**, 2419–2422.
- 23 S. Mimmi, D. Maisano, N. Nisticò, E. Vecchio, F. Chiurazzi, K. Ferrara, M. Iannalfo, A. D'Ambrosio, G. Fiume, E. Iaccino and I. Quinto, Detection of chronic lymphocytic leukemia subpopulations in peripheral blood by phage ligands of tumor immunoglobulin B cell receptors, *Leukemia*, 2021, **35**, 610–614.
- 24 A. W. Harris, C. A. Pinkert, M. Crawford, W. Y. Langdon, R. L. Brinster and J. M. Adams, The E mu-myc transgenic mouse. A model for high-incidence spontaneous lymphoma and leukemia of early B cells. The E mu-myc transgenic mouse. A model for high-incidence spontaneous lymphoma and leukemia of early B cells, *J. Exp. Med.*, 1988, **167**, 353–371.
- 25 S. B. Tuncer, D. Akdeniz, B. Celik, S. Kilic, O. Sukruoglu, M. Avsar, L. Ozer, M. Ekenel, S. Ozel and H. Yazici, The expression levels of miRNA-15a and miRNA-16-1 in circulating tumor cells of patients with diffuse large B-cell lymphoma, *Mol. Biol. Rep.*, 2019, **46**, 975–980.
- 26 M. Sasaki, T. Ishikawa, M. Ishiguro, S. Okazaki, S. Yamauchi, A. Kikuchi, T. Matsuyama, K. Kawada, M. Tokunaga, H. Uetake and Y. Kinugasa, The effectiveness of plasma miR-33a-5p as a predictive biomarker for the efficacy of colorectal cancer chemotherapy, *Oncol. Lett.*, 2021, **21**, 489.
- 27 P. Roth, A. Keller, J. D. Hoheisel, P. Codo, A. S. Bauer, C. Backes, P. Leidinger, E. Meese, E. Thiel, A. Korfel and M. Weller, Differentially regulated miRNAs as prognostic biomarkers in the blood of primary CNS lymphoma patients, *Eur. J. Cancer*, 2015, **51**, 382–390.